

MODEL BASED PREDICTIVE CONTROL OF AN AIRCRAFT WITH ACTUATOR FAILURE IN A TERRAIN FOLLOWING TASK

Gustavo Lima Carneiro, gustavolc@gmail.com

Instituto Tecnológico de Aeronáutica - ITA, Divisão de Engenharia Mecânica-Aeronáutica

Roberto Kawakami Harrop Galvão, kawakami@ita.br

Instituto Tecnológico de Aeronáutica - ITA, Divisão de Engenharia Eletrônica

Abstract. *This paper concerns the application of model-based predictive control to the longitudinal mode of an aircraft in a terrain following task. The predictive control approach was based on a quadratic cost function and a linear state-space prediction model with input and state constraints. The optimal control was obtained as the solution of a quadratic programming problem defined over a receding horizon. Closed-loop simulations were carried out by using the nonlinear aircraft model. An elevator actuator failure was introduced in order to analyze the controller performance in the presence of tighter input constraints. The results show that predictive control may be an adequate alternative for terrain following tasks, especially if the input constraints become more strict as the result of an actuator failure.*

Keywords: *Model-based predictive control, Optimization, Terrain following, Fault-tolerant control.*

1. INTRODUCTION

Model (Based) Predictive Control (MPC) is a control methodology that has been applied with significant impact on industrial plants, specially in cases involving inputs and state constraints. The essence of MPC is to optimize, over the manipulated inputs, forecasts of process behavior. Classical control strategies (such as PID, for instance) normally do not explicitly consider the future implications of the current control action. To some extent this is accounted for by the expected closed-loop dynamics. MPC, on the other hand, explicitly computes the predicted behavior over some time horizon. The term MPC, in reality, designates a wide range of control methods that make use of a process model in order to obtain the optimal control value by minimizing a cost function. MPC algorithms differ among themselves mainly due to the model used to represent the process being controlled, the representation of measurement noise and exogenous disturbances, and the objective function to be minimized (Camacho; Bordons, 2000).

MPC can be used to control a great variety of processes, including systems with non-minimum phase or unstable dynamics. Additionally, it handles actuator constraints in a systematic form and intrinsically provides compensation for dead times (Camacho, Bordons, 2000), (Maciejowski, 2002). One disadvantage of such a methodology concerns the computational effort required, as the control actions are obtained by solving a dynamic optimization problem in real time. However, the greatest drawback when compared to the traditional control methodologies is the need for an appropriate model of the process to be available (Camacho; Bordons, 2000).

Predictive control has been applied to a wide range of areas, especially those related to process industry. Chemical industry, for instance, has adopted predictive control strategies due to the simplicity of algorithms based on step response models of the process. The petrochemical sector has also used predictive control approaches since the eighties as reported by (Camacho; Bordons, 2000). Other applications of predictive control schema can be found in robot manipulators, clinical anesthesia equipment and PVC plants, among others. Regarding high bandwidth applications, such as aeronautics and space, MPC has only recently been studied as a suitable control approach, due to the growth of the processing capability of computational resources, in special with respect to Flight Control Systems (FCS). For example, to extend MPC applications to miniaturized devices and/or embedded systems, the implementation of this control technology has been explored into reconfigurable hardware such as FPGA chips (Ling; Yue; Maciejowski, 2006).

Several studies have been conducted to better understand the applicability and feasibility of Predictive Control to the aircraft FCS. In this context, MPC has been reported as a possible control strategy for a super maneuverable aircraft (Maciejowski; Heise, 1996). A fault tolerance analysis was accomplished for a high performance aerospace system which makes use of MPC with the objective of demonstrating its effectiveness in handling control surface failures (EBDON; HEISE, 1997). An XV-15 Tilt Rotor Control study using MPC was performed as well as the implementation on a real time simulator (MEHRA et al., 2001). A Flight Control System for a Reusable Launch Vehicle based on MPC can be found and has demonstrated, among other results, the potential of MPC for reconfigurable control (Miotto; Lepome, 2003).

In the present paper, the potential advantages of using MPC as the Flight Control System for an aircraft performing a Terrain Following task are investigated. Such a task consists of tracking the ground profile, over a predetermined height. It is primarily used by military aircraft (mainly fighters) to enable flight at low altitude and high speed. The main objective of such unusual trajectory is to provide low radar signature, thus avoiding detection by anti-aircraft systems. Since pilots would not be able to react to changes in terrain profile in a timely manner, it is necessary to

provide terrain-following radar supporting a combined flight control system. However, limitations on time of response, load factor or even weather conditions may impose constraints on how low and fast an aircraft can perform a flight.

Terrain Following Problem (TFP) comprises trajectory planning and trajectory tracking, where the first is related to the generation of reference trajectory that follows a predetermined terrain (satisfying mission requirements and performance constraints) and the second involving a task for FCS, which ensures that the system will follow, with some precision, the flight path in the presence of external disturbances. Several approaches have been developed to deal with TFP. The longitudinal motion of aircraft is normally considered despite the fact that better terrain following could be achieved using both longitudinal and lateral-directional trajectory, specially dealing with maneuvers performed to avoid collision (Williams, 2005).

The present work involves a simplified nonlinear model for the longitudinal dynamics of a fighter aircraft. The prediction model to be used in the controller is obtained by linearization of the state equations around an equilibrium point. Closed-loop simulations are carried out in the Matlab-Simulink environment. The results show that the controller is capable of providing adequate tracking of the terrain profile with proper handling of input and state constraints. In addition, appropriate performance is maintained in the presence of an actuator failure that restricts the excursion of the elevator.

The remaining sections of this paper are organized as follows. Section 2 presents the MPC formulation adopted in this work. Section 3 describes the aircraft model employed in the case study. Section 4 presents the parameters adopted in the simulations. Section 5 reports the results and discusses the potential advantages of using MPC in the scenarios under consideration. Finally, concluding remarks are given in Section 6.

2. CONSTRAINED MODEL BASED PREDICTIVE CONTROL

The MPC controller aims to calculate the optimal control actions by minimizing a given cost function. When the system is unconstrained, a closed form mathematical solution may be derived. However, when active constraints are present, the solution must be obtained by using numerical optimization techniques (Miotto and Lepome, 2003). The constrained case will be covered herein.

Consider a system of order n , with p inputs and q outputs, with the discrete state space representation given by Eq. (1) and (2).

$$\mathbf{x}(k+1) = \mathbf{A}\mathbf{x}(k) + \mathbf{B}\mathbf{u}(k) \quad (1)$$

$$\mathbf{y}(k) = \mathbf{C}\mathbf{x}(k) \quad (2)$$

where $k \in \mathbb{Z}^+$ is the discrete time index, $\mathbf{x} \in \mathbb{R}^n$ represents the state vector, $\mathbf{u} \in \mathbb{R}^p$ is the input vector and $\mathbf{y} \in \mathbb{R}^q$ is the output vector. The state, input and output matrices are denoted by \mathbf{A} , \mathbf{B} and \mathbf{C} , respectively. The state space model is used to predict the behavior of the plant, starting at the current time, over a future prediction horizon. Control inputs are calculated by minimizing a cost function and, at the same time, enforcing the system constraints. The cost function chosen, expressed in Eq. (3), has a quadratic form and involves both the error values (difference between the reference trajectory and the predicted output) and control signal variations.

$$J = (\hat{\mathbf{Y}} - \mathbf{R})^T \mathbf{W}_y (\hat{\mathbf{Y}} - \mathbf{R}) + \Delta \hat{\mathbf{U}}^T \mathbf{W}_u \Delta \hat{\mathbf{U}} \quad (3)$$

In Eq. (3), J is the cost function value, $\hat{\mathbf{Y}}$ represents the predicted output vector, \mathbf{R} is the reference vector and $\Delta \hat{\mathbf{U}}$ is the vector of predicted control variations. These parameters are defined in Eq. (4). \mathbf{W}_y and \mathbf{W}_u are the weight matrices for the error and control variation values and are given by Eq. (5) and (6).

$$\hat{\mathbf{Y}} = \begin{bmatrix} \hat{y}(k+1|k) \\ \hat{y}(k+2|k) \\ \vdots \\ \hat{y}(k+H_p|k) \end{bmatrix} \quad \mathbf{R} = \begin{bmatrix} R(k+1|k) \\ R(k+2|k) \\ \vdots \\ R(k+H_p|k) \end{bmatrix} \quad \Delta \hat{\mathbf{U}} = \begin{bmatrix} \Delta \hat{u}(k|k) \\ \Delta \hat{u}(k+1|k) \\ \vdots \\ \Delta \hat{u}(k+H_u-1|k) \end{bmatrix} \quad (4)$$

$$\mathbf{W}_y = \begin{bmatrix} \Sigma(\mu) & 0_{q \times q} & \cdots & 0_{q \times q} \\ 0_{q \times q} & \Sigma(\mu) & \cdots & 0_{q \times q} \\ \vdots & \vdots & \ddots & \vdots \\ 0_{q \times q} & 0_{q \times q} & \cdots & \Sigma(\mu) \end{bmatrix} \quad \mathbf{W}_u = \begin{bmatrix} \Sigma(\rho) & 0_{p \times p} & \cdots & 0_{p \times p} \\ 0_{p \times p} & \Sigma(\rho) & \cdots & 0_{p \times p} \\ \vdots & \vdots & \ddots & \vdots \\ 0_{p \times p} & 0_{p \times p} & \cdots & \Sigma(\rho) \end{bmatrix} \quad (5)$$

$$\Sigma(\mu) = \begin{bmatrix} \mu_1 & 0 & \cdots & 0 \\ 0 & \mu_2 & \cdots & 0 \\ \vdots & \vdots & \ddots & \vdots \\ 0 & 0 & \cdots & \mu_q \end{bmatrix} \quad \Sigma(\rho) = \begin{bmatrix} \rho_1 & 0 & \cdots & 0 \\ 0 & \rho_2 & \cdots & 0 \\ \vdots & \vdots & \ddots & \vdots \\ 0 & 0 & \cdots & \rho_p \end{bmatrix} \quad (6)$$

The predicted values for the output, $\hat{y}(k+i/k)$, are obtained from the state space model at the time k . The parameter H_p represents the prediction horizon, which determines the extension of the prediction in terms of the quantity of sample periods (T_s). The predicted control variations, $\Delta\hat{u}(k+i/k)$, represent the change of the control signal referred to the previous sample period. They are obtained for a control horizon, H_u , which is usually smaller than the prediction horizon (i.e., $H_u < H_p$). This leads the minimization to work over a smaller number of variables, diminishing the demanded computational effort. After the minimization of the cost function has achieved the best control variations, just the first value is used, i.e. $\Delta u(k) = \Delta\hat{u}^*(k/k)$.

The state space model (Eq.(1) and (2)) can be used to rewrite the cost function (Eq. (3)) by expressing $\hat{\mathbf{Y}}$ in terms of $\Delta\hat{\mathbf{U}}$ as

$$\hat{\mathbf{Y}} = \mathbf{G}\Delta\hat{\mathbf{U}} + \mathbf{F} \quad (7)$$

where \mathbf{G} accounts for the matrix that, multiplied by the predicted control variations, yields the additional system response to the control movements over the prediction horizon and \mathbf{F} is the system response vector when applying only the inputs of the previous sampling instant. \mathbf{G} and \mathbf{F} are given by Eq. (8) and result from grouping the terms after iterating state space model for the H_p sampling periods, to obtain the predicted system response as a function of the predicted control variations, $\Delta\hat{\mathbf{U}}$. Eq. (9) and (10) present the terms that constitute \mathbf{G} and \mathbf{F} .

$$\mathbf{G} = \mathbf{T}_{H_p}^{I_q} \mathbf{P} \quad \mathbf{F} = \mathbf{T}_{H_p}^{I_q} \mathbf{Q}\Delta\mathbf{x}(k) + \Gamma_q \mathbf{y}(k) \quad (8)$$

$$\mathbf{T}_{H_p}^{I_q} = \begin{bmatrix} \mathbf{I}_q & 0 & \cdots & 0 \\ \mathbf{I}_q & \mathbf{I}_q & \cdots & 0 \\ \vdots & \vdots & \ddots & \vdots \\ \mathbf{I}_q & \mathbf{I}_q & \cdots & \mathbf{I}_q \end{bmatrix} \quad \mathbf{P} = \begin{bmatrix} \mathbf{CB} & 0 & \cdots & 0 \\ \mathbf{CAB} & \mathbf{CB} & \cdots & 0 \\ \vdots & \vdots & \ddots & \vdots \\ \mathbf{CA}^{H_p-1} \mathbf{B} & \mathbf{CA}^{H_p-2} \mathbf{B} & \cdots & \mathbf{CA}^{H_p-H_u} \mathbf{B} \end{bmatrix} \quad (9)$$

$$\mathbf{Q} = \begin{bmatrix} \mathbf{CA} \\ \mathbf{CA}^2 \\ \vdots \\ \mathbf{CA}^{H_p} \end{bmatrix} \quad \Gamma_q = \begin{bmatrix} \mathbf{I}_q \\ \mathbf{I}_q \\ \vdots \\ \mathbf{I}_q \end{bmatrix} \quad (10)$$

In Eq. (8), (9) and (10), $\Delta\mathbf{x}(k)$ is the state variation vector referred to the previous sample time and \mathbf{I}_q is the $q \times q$ identity matrix. By replacing Eq. (7) into (3), one obtains Eq. (11), which is a quadratic expression in terms of $\Delta\hat{\mathbf{U}}$.

$$J(\Delta\hat{\mathbf{U}}) = \frac{1}{2} (\Delta\hat{\mathbf{U}})^T \boldsymbol{\eta} (\Delta\hat{\mathbf{U}}) + \mathbf{f}^T \Delta\hat{\mathbf{U}} + c \quad (11)$$

where $\boldsymbol{\eta}$, \mathbf{f} and c are given by Eq. (12).

$$\boldsymbol{\eta} = 2(\mathbf{G}^T \mathbf{W}_y \mathbf{G} + \mathbf{W}_u) \quad \mathbf{f} = 2\mathbf{G}^T \mathbf{W}_y (\mathbf{F} - \mathbf{R}) \quad c = (\mathbf{F} - \mathbf{R})^T \mathbf{W}_y (\mathbf{F} - \mathbf{R}) \quad (12)$$

In the absence of restrictions over the inputs, outputs or states, the vector that minimizes J (Eq. (11)) can be obtained by calculating the gradient for J and making it equal to zero (Eq. (13)).

$$\frac{\partial J}{\partial \Delta \hat{\mathbf{U}}} = \Delta \hat{\mathbf{U}}^T \boldsymbol{\eta} + \mathbf{f}^T = 0 \quad \Delta \hat{\mathbf{U}}^* = -\boldsymbol{\eta}^{-1} \mathbf{f} \quad (13)$$

where $\Delta \hat{\mathbf{U}}^*$ denotes the vector of input changes that minimizes the cost function value.

In the presence of system restrictions representing constraints over the inputs (or input variations), states or outputs, this algebraic solution may not be admissible. In this case, the optimal control can be obtained as the solution of a Quadratic Programming (or QP) problem, for which standard algorithms are available. The restrictions for the inputs, states and outputs will be considered as upper and lower limits for their values and are expressed in Eq. (14) and (15).

$$\begin{bmatrix} \Delta \mathbf{u}_{\min} \\ \Delta \mathbf{u}_{\min} \\ \vdots \\ \Delta \mathbf{u}_{\min} \end{bmatrix} \leq \begin{bmatrix} \Delta \hat{\mathbf{u}}(k/k) \\ \Delta \hat{\mathbf{u}}(k+1/k) \\ \vdots \\ \Delta \hat{\mathbf{u}}(k+H_u-1/k) \end{bmatrix} \leq \begin{bmatrix} \Delta \mathbf{u}_{\max} \\ \Delta \mathbf{u}_{\max} \\ \vdots \\ \Delta \mathbf{u}_{\max} \end{bmatrix} \quad \begin{bmatrix} \mathbf{u}_{\min} \\ \mathbf{u}_{\min} \\ \vdots \\ \mathbf{u}_{\min} \end{bmatrix} \leq \begin{bmatrix} \hat{\mathbf{u}}(k/k) \\ \hat{\mathbf{u}}(k+1/k) \\ \vdots \\ \hat{\mathbf{u}}(k+H_u-1/k) \end{bmatrix} \leq \begin{bmatrix} \mathbf{u}_{\max} \\ \mathbf{u}_{\max} \\ \vdots \\ \mathbf{u}_{\max} \end{bmatrix} \quad (14)$$

$$\begin{bmatrix} \mathbf{x}_{\min} \\ \mathbf{x}_{\min} \\ \vdots \\ \mathbf{x}_{\min} \end{bmatrix} \leq \begin{bmatrix} \hat{\mathbf{x}}(k+1/k) \\ \hat{\mathbf{x}}(k+2/k) \\ \vdots \\ \hat{\mathbf{x}}(k+H_p/k) \end{bmatrix} \leq \begin{bmatrix} \mathbf{x}_{\max} \\ \mathbf{x}_{\max} \\ \vdots \\ \mathbf{x}_{\max} \end{bmatrix} \quad \begin{bmatrix} \mathbf{y}_{\min} \\ \mathbf{y}_{\min} \\ \vdots \\ \mathbf{y}_{\min} \end{bmatrix} \leq \begin{bmatrix} \hat{\mathbf{y}}(k+1/k) \\ \hat{\mathbf{y}}(k+2/k) \\ \vdots \\ \hat{\mathbf{y}}(k+H_p/k) \end{bmatrix} \leq \begin{bmatrix} \mathbf{y}_{\max} \\ \mathbf{y}_{\max} \\ \vdots \\ \mathbf{y}_{\max} \end{bmatrix} \quad (15)$$

The set of constraints can be expressed by inequalities involving $\Delta \hat{\mathbf{U}}$, as summarized by (16).

$$\begin{bmatrix} \mathbf{I}_{pH_u} \\ -\mathbf{I}_{pH_u} \\ \mathbf{T}_{H_u}^I \\ -\mathbf{T}_{H_u}^I \\ \mathbf{K}_{AB} \\ -\mathbf{K}_{AB} \\ \mathbf{G} \\ -\mathbf{G} \end{bmatrix} \Delta \hat{\mathbf{U}} \leq \begin{bmatrix} \Lambda_{H_u} [\Delta \mathbf{u}_{\max}] \\ -\Lambda_{H_u} [\Delta \mathbf{u}_{\min}] \\ \Lambda_{H_u} [\mathbf{u}_{\max}] \\ -\Lambda_{H_u} [\mathbf{u}_{\min}] \\ \Lambda_{H_p} [\mathbf{x}_{\max} - \mathbf{K}_A \mathbf{x}(k) - \mathbf{K}_B \mathbf{u}(k-1)] \\ \Lambda_{H_p} [\mathbf{x}_{\min} + \mathbf{K}_A \mathbf{x}(k) + \mathbf{K}_B \mathbf{u}(k-1)] \\ \Lambda_{H_p} [\mathbf{y}_{\max}] - \mathbf{F} \\ \mathbf{F} - \Lambda_{H_p} [\mathbf{y}_{\min}] \end{bmatrix} \quad (16)$$

where \mathbf{I}_{pH_u} denotes the $(pH_u \times pH_u)$ identity matrix and the operator “ $\Lambda_i[\]$ ” creates an $(i \times 1)$ vector of its argument. Matrices \mathbf{K}_A , \mathbf{K}_B and \mathbf{K}_{AB} are given by Eq. (17).

$$\mathbf{K}_A = \begin{bmatrix} \mathbf{A} \\ \vdots \\ \mathbf{A}^{Hu} \\ \mathbf{A}^{Hu+1} \\ \vdots \\ \mathbf{A}^{Hp} \end{bmatrix} \quad \mathbf{K}_B = \begin{bmatrix} \mathbf{B} \\ \vdots \\ \sum_{i=0}^{i=H_u-1} \mathbf{A}^i \mathbf{B} \\ \sum_{i=0}^{i=H_u} \mathbf{A}^i \mathbf{B} \\ \vdots \\ \sum_{i=0}^{i=H_p-1} \mathbf{A}^i \mathbf{B} \end{bmatrix} \quad \mathbf{K}_{AB} = \begin{bmatrix} \mathbf{B} & \dots & 0 \\ \mathbf{AB} + \mathbf{B} & \dots & 0 \\ \vdots & \ddots & \vdots \\ \sum_{i=0}^{i=H_u-1} \mathbf{A}^i \mathbf{B} & \dots & \mathbf{B} \\ \sum_{i=0}^{i=H_u} \mathbf{A}^i \mathbf{B} & \dots & \mathbf{AB} + \mathbf{B} \\ \vdots & \vdots & \vdots \\ \sum_{i=0}^{i=H_p-1} \mathbf{A}^i \mathbf{B} & \dots & \sum_{i=0}^{i=H_p-H_u} \mathbf{A}^i \mathbf{B} \end{bmatrix} \quad (17)$$

3. AIRCRAFT LONGITUDINAL DYNAMICS

The description of the aircraft flight dynamics essentially aims to determine the forces and moments to which it is subjected to and then obtain, as a result, its acceleration, velocity and position as a function of the time. For this paper, the dynamic will be expressed with the application of Newton's Second Law for both translational and rotational movement, with an ultimate interest in the aircraft longitudinal mode. Aircraft control means, simplistically, to somehow manipulate the applied forces or moments to cause acceleration to change in a way that yields the desired position and velocity. Typically these forces and moments will be from aerodynamic and propulsive origin, and the usual controls are elevators (or elevons), ailerons, rudders, canards, flaps, spoilers and slats. They act to change the local pressure distribution and hence the aerodynamic forces and moments (Durham, 1997).

The external forces that accelerate an aircraft are made up of its weight \mathbf{W} , the aerodynamic resultant force \mathbf{R}_A and the thrust of the propulsive system, \mathbf{T} , and are given by Eq. (18) (Body-axis reference frame used). The forces that actuate through the Y-body axis are being neglected, therefore, no latero-directional movement is under analysis.

$$\{\mathbf{W}\}_B = \begin{bmatrix} -mg \sin(\theta) \\ 0 \\ mg \cos(\theta) \end{bmatrix} \quad \{\mathbf{R}_A\}_B = \begin{bmatrix} X \\ 0 \\ Z \end{bmatrix} \quad \{\mathbf{T}\}_B = \begin{bmatrix} T \cos(\alpha_T) \\ 0 \\ T \sin(\alpha_T) \end{bmatrix} \quad (18)$$

where m is the aircraft mass, g is the gravity, θ is the pitch angle, X and Z are components of aerodynamic force (expressed in the body reference frame), T is the thrust modulus and α_T is the angle between the thrust vector and the X-body axis. In terms of moments and taking as the reference the aircraft CG point, the weight force does not generate any moment around it, since it acts through the Center of Gravity. Only the moment generated by the aerodynamic and propulsive forces are considered. The aerodynamic moment about the CG, denoted as \mathbf{M}_A and the thrust generated moment, referred as \mathbf{M}_T , are represented in the Body reference frame by Eq. (19).

$$\{\mathbf{M}_A\}_B = \begin{bmatrix} 0 \\ m_a \\ 0 \end{bmatrix} \quad \{\mathbf{M}_T\}_B = \begin{bmatrix} 0 \\ m_T \\ 0 \end{bmatrix} \quad (19)$$

3.1 Forces and Moment Equations

The aerodynamic forces and moments acting on the aircraft can be defined in terms of the dynamic pressure \bar{q} , a characteristic area S , a characteristic length b , and dimensionless aerodynamic coefficients. Propulsive force is obtained by a simplified model, which considers the dependence from the thrust into basically the velocity of the air and its density. Forces, moment and dynamic pressure equations are given by Eq. (20).

$$X = \bar{q} S C_X \quad Z = \bar{q} S C_Z \quad m_A = \bar{q} S b C_m \quad \bar{q} = \frac{1}{2} \rho V^2 \quad T = \delta_{th} F_{\max} \left(\frac{V}{V_r} \right)^{m_v} \left(\frac{\rho}{\rho_r} \right)^{m_r} \quad (20)$$

where ρ is the air density and V is the velocity modulus. The force coefficients C_X and C_Z are obtained from C_L and C_D , aerodynamic coefficients derived from the forces described in wind axis representation. They are promptly obtained by

the suitable transformation from wind to body axis. Force and moment dimensionless coefficients are given by Eq. (21) and (22).

$$C_L = C_{L_0} + C_{L_\alpha} \alpha + C_{L_{\delta_e}} \delta_e + C_{L_q} \frac{qc}{V_e} \quad C_D = C_{D_0} + K_1 C_L + K_2 C_L^2 \quad (21)$$

$$C_m = C_{m_0} + C_{m_\alpha} \alpha + C_{m_{\delta_e}} \delta_e + (C_{m_q} q + C_{m_{\dot{\alpha}}} \dot{\alpha}) \frac{c}{V_e} \quad (22)$$

3.2 Equations of Motion

The equations of motion are the differential equations that describe the evolution of the most commonly represented states of an aircraft: the scalar components of the velocity, the position vector components, the orientation or Euler angles, etc. Given the translational and rotational velocity vectors (here denoted as \mathbf{V} and $\boldsymbol{\omega}$, respectively, presented in Eq. (23)), the differential equations for their components follows as expressed by Eq. (24).

$$\{\mathbf{V}\}_B = [u \quad v \quad w]^T \quad \{\boldsymbol{\omega}\}_B = [p \quad q \quad r]^T \quad (23)$$

$$\dot{u} = \frac{X+T \cos(\alpha_T)}{m} - g \sin(\theta) - qw \quad \dot{w} = \frac{Z+T \sin(\alpha_T)}{m} + g \cos(\theta) + qu \quad \dot{q} = \frac{m_R}{I_y} \quad (24)$$

where m_R is the resultant moment acting on the aircraft and I_y is the moment of inertia around Y-body axis. Other important differential equations are presented in Eq. (25), where α is the angle of attack and z is the altitude.

$$\dot{\theta} = q \quad \dot{\alpha} = \frac{u\dot{w} + w\dot{u}}{u^2 + w^2} \quad \dot{z} = u \sin(\theta) + w \cos(\theta) \quad (25)$$

4. SIMULATIONS

In the simulations, the state vector \mathbf{x} was defined as $[V \alpha \theta q H]^T$. The control inputs were the throttle setting and elevator actuator deflection, represented by $[\delta_h \delta_e]^T$. First order filters were used as the engine and elevator actuator dynamics and were considered in both the non-linear and linearized state space representations. The time constants are, respectively, $\tau_{eng} = 5$ and $\tau_{elev} = 0.0495$ seconds. Linearization was obtained for a flight condition with airspeed velocity of 100 m/s, 500 m of altitude, resulting in equilibrium control inputs of [0.334 -0.0649]. Matlab / Simulink environment was used to obtain the results. The MPC parameters adopted in the simulation are found in Tab. 1.

Table 1. Predictive controller parameters.

Parameter	Value	Unit
T_s	0.3	sec
H_p	50	sample periods
H_u	20	sample periods
μ	18	1/m ²
$[\rho_1, \rho_2]$	[25 20]	[- 1/rad ²]

Initially, the constraints were defined for the inputs and states, except for the state H , whose lower bound constraints were established on the basis of the terrain database passed to the controller. Inequality (26) shows the values chosen for such constraints, considering it as deviations with respect to the equilibrium values. After the actuator failure, which limited its maximum excursion to $\pm 5^\circ$, the constraints represented by (27) were considered inside the controller.

$$\begin{bmatrix} -30 \text{ m/s} \\ -0.1717 \text{ rad} \\ -0.7854 \text{ rad} \\ -1.047 \text{ rad/s} \end{bmatrix} \leq \begin{bmatrix} V \\ \alpha \\ \theta \\ q \end{bmatrix} \leq \begin{bmatrix} 30 \text{ m/s} \\ 0.8755 \text{ rad} \\ 0.7854 \text{ rad} \\ 1.047 \text{ rad/s} \end{bmatrix} \quad \begin{bmatrix} -0.3342 \\ -0.3715 \text{ rad} \end{bmatrix} \leq \begin{bmatrix} \delta_h \\ \delta_e \end{bmatrix} \leq \begin{bmatrix} 0.6658 \\ 0.5012 \text{ rad} \end{bmatrix} \quad (26)$$

$$\begin{bmatrix} -0.3342 \\ -0.0224 \text{ rad} \end{bmatrix} \leq \begin{bmatrix} \delta_{th} \\ \delta_e \end{bmatrix} \leq \begin{bmatrix} 0.6658 \\ 0.1522 \text{ rad} \end{bmatrix} \quad (27)$$

In order to make predictive controller aware about the new elevator actuator constraints, a failure detection and diagnostic module would be necessary.

The *quadprog* function, from Matlab Optimization Toolbox, was used to calculate the solution of the QP problem in the simulations. The *Medium Scale Quadprog Algorithm* was used, which is an active-set strategy also known as a projection method (Mathworks, 2009). Based on the terrain following task, the reference trajectory was obtained with a terrain database, which contains only information about the ground profile and does not include the height of trees or buildings. An altitude clearance of 50 meters above the ground was assumed. Therefore, the output set-point was chosen as the terrain profile added to the clearance value.

5. RESULTS

Figure 1 presents the aircraft response considering a fault which restricted the elevator actuator excursion. The fault was inserted during the simulation after 39 km of distance. As can be seen, the aircraft was able to continue tracking the terrain reference with error values very similar to the system with nominal excursion for the elevator actuator. The maximum errors reached approximately 40 m above or below the reference trajectory which did not cause the aircraft to collapse with the ground in any instant. In other words, the constraint for the altitude was enforced by the controller. For relatively constant terrain reference, which can be noted between 23 and 30 km, the error was practically driven to zero. The points with higher error values were observed to be those with highly abrupt terrain variations. Figure 3 shows the values obtained for the velocity, angle of attack, pitch angle and pitch rate. It can be observed that the velocity reached higher values after the actuator failure, with an average value of almost 120 m/s.

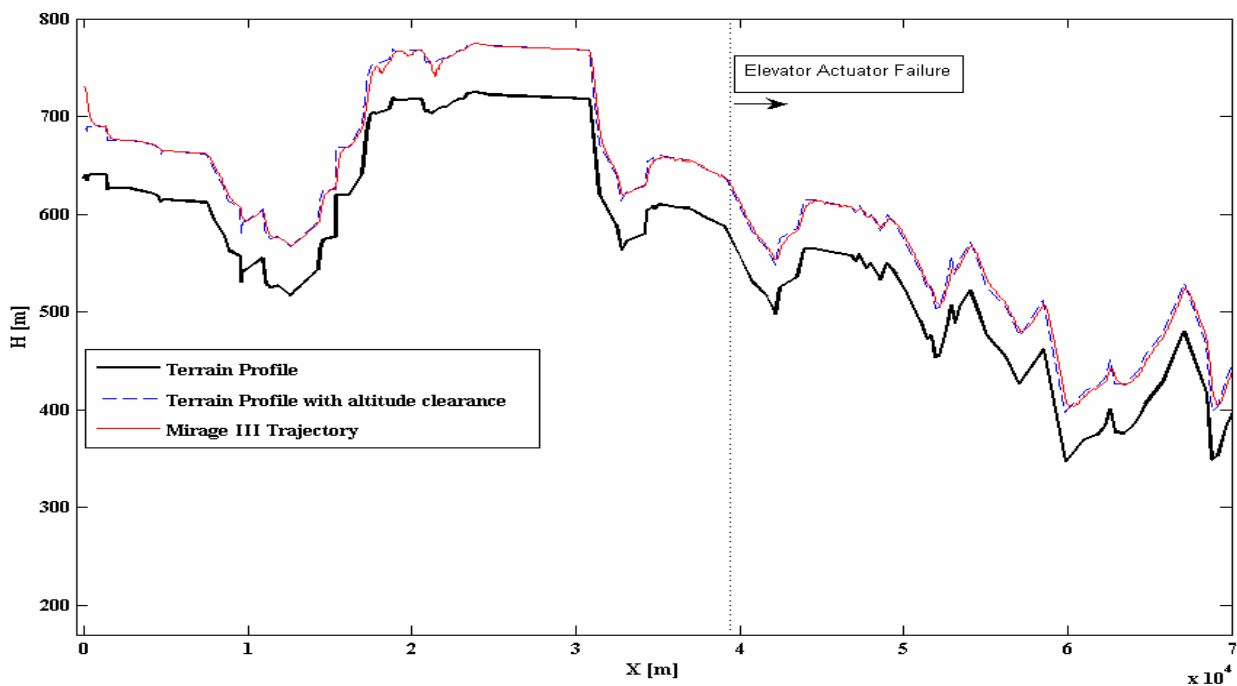


Figure 1. Aircraft altitude trajectory obtained for the terrain following task considering actuator excursion restraint.

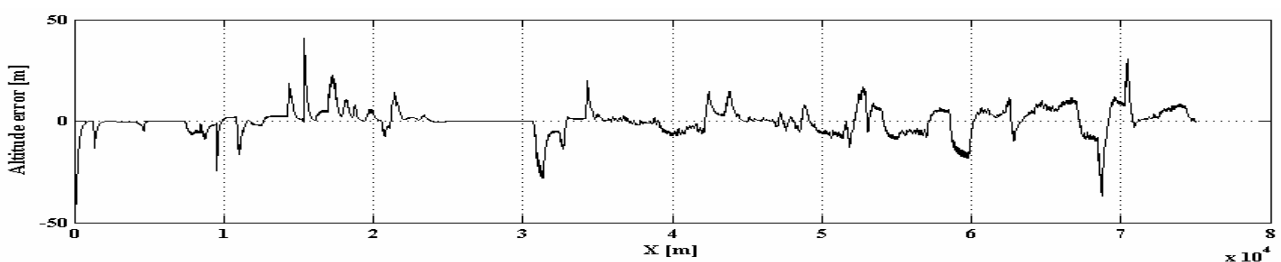


Figure 2. Aircraft altitude error.

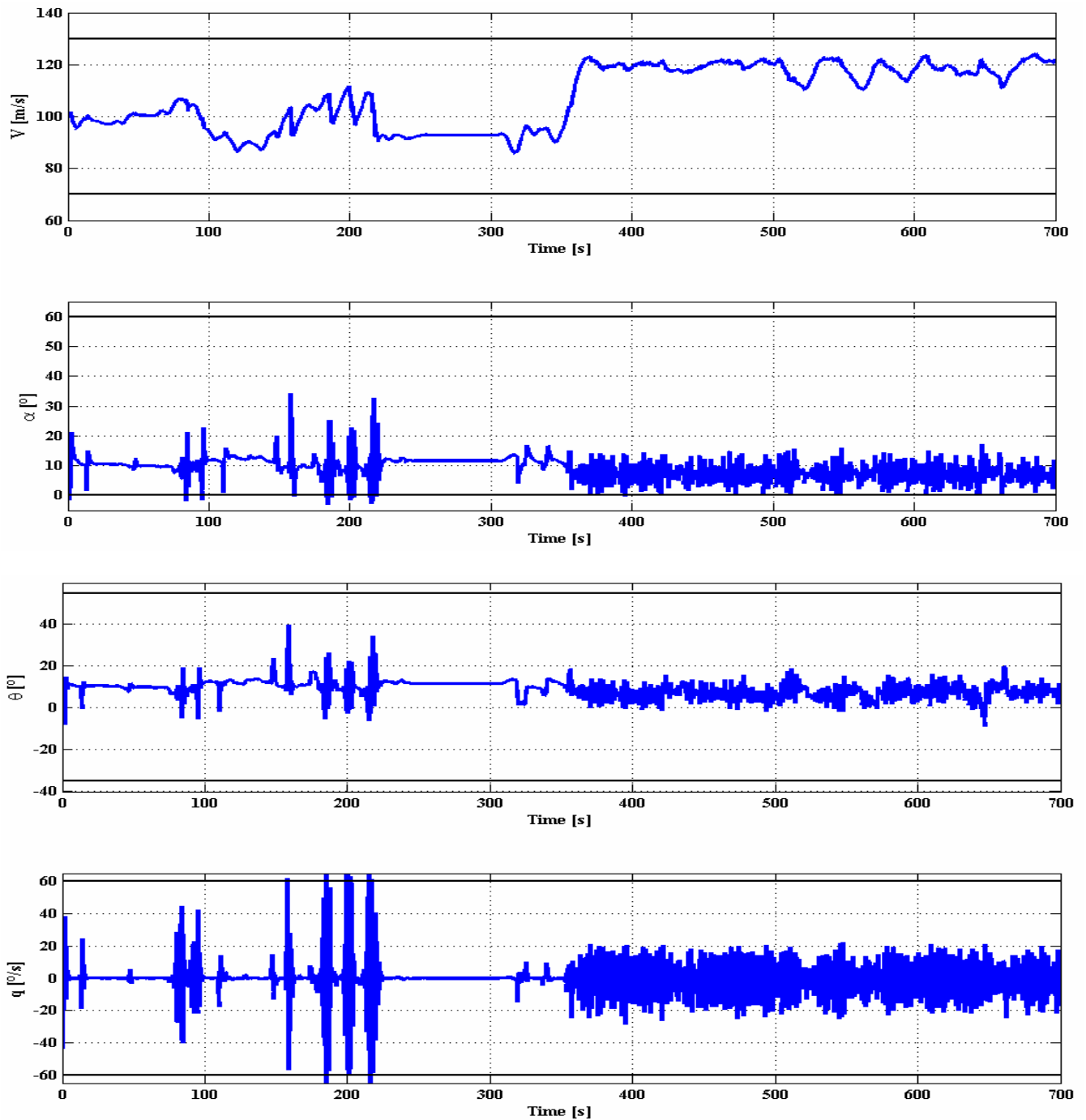


Figure 3. States velocity V , angle of attack α , pitch angle θ and pitch rate q obtained in the simulation.

This behavior arises due to two aspects: first of all, to obtain the same lift force in the elevator surface and associated pitch moment with the constrained actuator, the airspeed needs to be larger, in order to obtain a higher dynamic pressure. In fact, the lift coefficient is more limited with an excursion constraint for the elevator actuator. The other point to be emphasized is that now the main control that can provide altitude variation is the thrust. As the propulsive force is used more intensely it causes changes in the aircraft velocity, increasing it, and therefore, leading to higher lift force.

Prior to the actuator failure, the angle of attack stayed within the limits imposed by the constraints for the majority of the simulation time. In some points, the angle of attack decreased to less than the minimal value allowed. The reasons for this violation are two-fold. Firstly, the aircraft is flying with significant deviation from the point where the linear model was obtained. Therefore, the predictions present errors with respect to the actual output of the non-linear model. Such prediction errors can lead to control values that drive the aircraft to go beyond the allowable limits. Secondly, the

algorithm finds the minimization infeasible in some points. As a result, the optimization outcome is out of the control input range, but it is still sent to the plant actuators as commands. Control signal saturation is applied *a posteriori*, to the throttle setting and elevator surface deflection. Regarding the pitch angle, it can be observed that it stayed within the established limits. The maneuvers were performed with more than -10° and up to 40° . For pitch rate, the limits were briefly violated for some instants as with the angle of attack.

After the actuator failure, the angle of attack and the pitch rate presented a more oscillatory behavior. As can be seen, the predictive controller was able to keep both variables within the limits imposed for the majority of the simulation time, even dealing with a more restricted excursion for the elevator actuator. The points corresponding to brief violation of the constraints are related to feasibility problems.

The control inputs generated by the predictive controller can be seen in Fig. 4. The elevator actuator excursion constraint led to an excessive demand of the throttle input, transferring to it the main control for the aircraft altitude, indirectly by the means of the velocity. This effect could be minimized by an online change of the weight inputs, increasing those related to the less constrained input. It can also be seen that the optimization was found to be infeasible at some sampling times and led to input excursions beyond the imposed limits for the algorithm. For these cases, several possibilities could be used to minimize the effects of such undesirable controller behavior. A possibility consists of using the control signal $\Delta \hat{\mathbf{u}}(k/k - 1)$ calculated in the previous sampling time. More sophisticated strategies try to relax the least important constraints in an attempt to regain feasibility (Maciejowski, 2002). For this case, a possible approach would be, for example, to allow a negative excursion for the angle of attack lower limitation, or to stretch the pitch rate constraints.

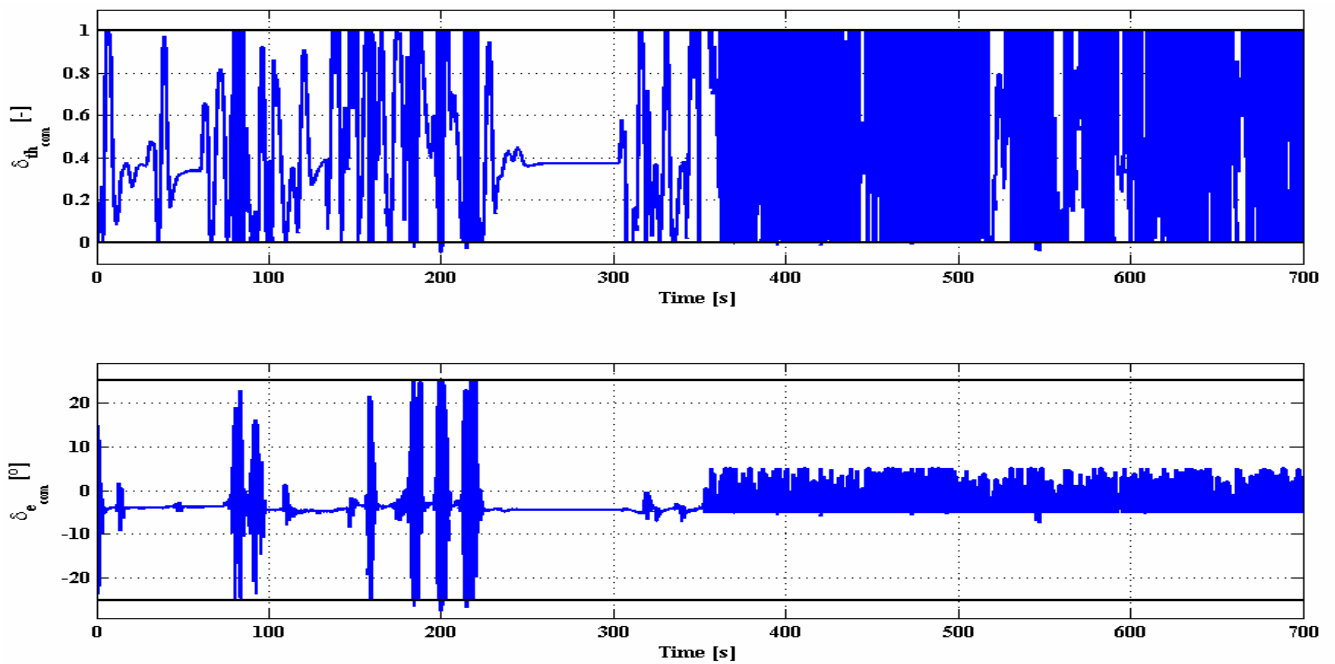


Figure 4. Commanded inputs $\delta_{th(com)}$ and $\delta_{e(com)}$.

The inputs sent to the aircraft through the actuators are presented in Fig. 5. Although the engine dynamics turn the system actuation slower, the predictive controller has already included it into the linear model which did help the system to provide the necessary thrust to perform the maneuvers and with reduced variations in the velocity value. For the elevator actuation, it practically followed the signal sent by the controller, as its dynamics is relatively fast. It has to be emphasized that the weight value chosen for the elevator input was observed to be quite suitable as it provided few points of full excursion for this actuator (prior to the elevator actuator failure).

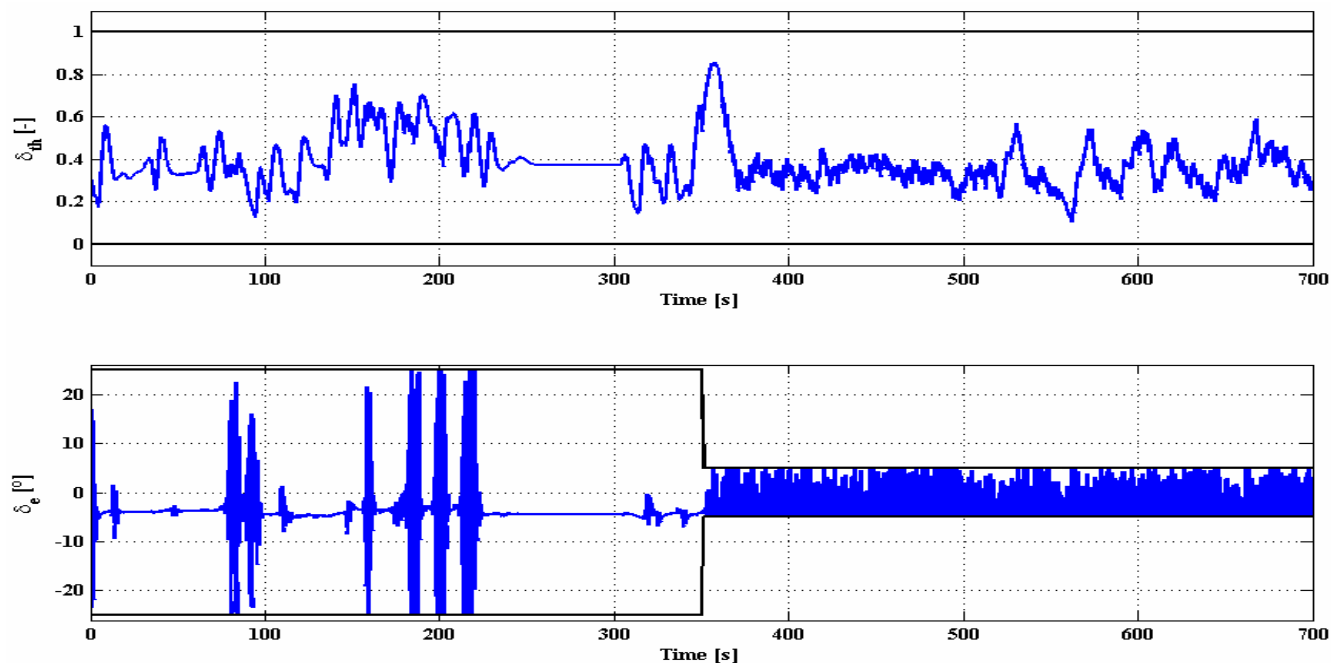


Figure 5. Inputs δ_{th} and δ_e effectively applied to the aircraft.

6. CONCLUSIONS

This paper presented an evaluation of a model based predictive controller used to control the aircraft altitude in the course of a terrain following task. A simplified non-linear model was used to simulate the system response. The predictive controller made use of a linearized state space representation in order to obtain the system predicted behavior for optimization purposes.

With the system running at its nominal constraints, the simulations showed that the predictive controller was a good approach to provide reference tracking for a terrain with strong altitude variations over its length. System constraints were in its majority respected during the simulation, except by some points in which the optimization algorithm found the problem to be infeasible. This infeasibility problem could be managed, for example, by on-line relaxation of the constraints. Upon the onset of a fault which restricted the excursion of the elevator actuator, the advantage of the predictive controller to deal with such a restraint was evident. In fact, good reference tracking and proper satisfaction of the constraints were preserved. Although the thrust input was much more demanded, the controller managed to keep the system state within the imposed limits.

7. REFERENCES

- Camacho, E. F.; Bordons, C., 2000, "Model Predictive Control". 2nd. ed. London: Springer.
- Durham, W. C., 1997, "Aircraft Dynamics and Control". 1st. ed. Virginia: Virginia Polytechnic Institute and State University.
- Ebdon, B. W.; Heise, S. A., 1997, "Model predictive control for fault tolerance in aerospace systems", American Institute of Aeronautics and Astronautics.
- Ling, K. V.; Yue, S. P.; Maciejowski, J. M., 2006, "A fpga implementation of model predictive control", Proceedings of the American Control Conference, Minneapolis.
- Maciejowski, J. M.; Heise, S. A., 1996, "Model predictive control of a supermaneuverable aircraft", American Institute of Aeronautics and Astronautics.
- Maciejowski, J. M., 2002, "Predictive Control with Constraints", 1st. ed., Harlow: Prentice Hall PTR.
- Mathworks, 2009, "Optimization Toolbox 4 User's Guide".
- Mehra, R. K.; Prasanth, R. K.; Bennet, R. L.; Wasikovski, M., 2001, "Model predictive control design for xv-15 tilt rotor flight control", American Institute of Aeronautics and Astronautics.
- Miotto, P.; Lepome, R. C., 2003., "Design of a model predictive control flight control system for a reusable launch vehicle", In: AIAA Guidance, Navigation, and Control Conference and Exhibit, Massachusetts.

8. RESPONSIBILITY NOTICE

The authors are the only responsible for the material included in this paper.